Available online at www.sciencedirect.com
SCIENCE DIRECT
Journal of Colloid and Interface Science 277 (2004) 327–334
JOURNAL OF Colloid and Interface Science
www.elsevier.com/locate/jcis

Reverse Monte Carlo modeling of the structure of colloidal aggregates

László Pusztai [a,*], Hector Dominguez [b], Orest A. Pizio [b]

[a] *Neutron Physics Laboratory, Research Institute for Solid State Physics and Optics, Hungarian Academy of Sciences, P.O.B. 49, Budapest H-1525, Hungary*

[b] *Instituto de Quimica UNAM, Circuito Exterior, Coyoacán 04510, D.F., Mexico*

Received 11 August 2003; accepted 23 April 2004

Available online 28 May 2004

Abstract

In this work we present results for the structure of aerogels coming from the diffusion-limited cluster aggregation simulation method. Pair distribution functions and structure factors, resulting from simulation, were considered as experimental input for reverse Monte Carlo modeling. The modeling yielded structural models with pair distribution functions and structure factors nearly identical to the results of the simulations. Particle configurations from both the simulations and reverse Monte Carlo modeling have been analyzed in terms of the distribution of the number of neighbors. It is suggested that the reverse Monte Carlo method, when applied to the structure factor, may be a suitable technique for the interpretation of experimental scattering data on colloidal aerogels.

Keywords: Aerogel; Structure; Computer simulation; Diffusion-limited cluster aggregation; Reverse Monte Carlo

1. Introduction

The microscopic (atomic level) structure of a material is undoubtedly its most basic property. Unfortunately, determining the microscopic structure of disordered (noncrystalline) systems, such as liquids and amorphous materials, is problematic, for there is no long-range ordering of well-defined structural units to rely on. This feature introduces difficulties during diffraction measurements, as well as during their interpretation. In general, these problems become greater if the structure of a disordered material is characterized by length scales that are larger than interatomic distances. However, important classes of materials such as gels and other disordered porous adsorbents fall into this category.

So far, studying the "structure" of such systems has almost exclusively meant considering the larger length scale only, with the notion that as far as the overall behavior of the system is concerned, the microscopic length scale is not relevant. In some cases, where the length scales are very different (say, by at least two orders of magnitude), this approach may be justified. Note that even then, the microscopic structure may be of interest on its own. Accordingly, the experimental methodology for investigating the different length scales is split: *diffraction* (X-ray or neutron) studies are aimed at the atomic level structure and *small-angle scattering* (SAS) [1] is the technique for looking at larger length scales. Although the underlying phenomena are very similar for diffraction and SAS (see, e.g., Ref. [2]), instrumentation and, especially, methods for interpreting results are rather different. On the other hand, there are a number of instances where the larger length scale does not exceed very much the interatomic distances, as in, for instance, some silica gels, or porous carbons [3]. In such systems, the nearly complete splitting described above is, to say the least, questionable, since one can only guess how important the coupling is between atomic and larger length scales. Another, related, issue is the way the microscopic structure is manifested in larger scale structural features. However, the knowledge of the microscopic structure is necessary to study adsorption or diffusion in porous materials. Experimental scattering techniques and methods for treating scattering data available at present do not make it possible to consider two different length scales simultaneously.

With this study, we wish to undertake structural studies that go beyond present practice: we will attempt the deter-

* Corresponding author. Fax: +36-1-392-2589.
E-mail address: lp@szfki.hu (L. Pusztai).

0021-9797/$ – see front matter
doi:10.1016/j.jcis.2004.04.041

mination of both the microscopic and mesoscopic structure by making large structural models that are consistent with experimental diffraction and SAS data. However, before attempting to consider real experimental data, it is necessary to validate our approach on model data which is free of systematic errors—and this is the main purpose of the present contribution.

A principal element of the scheme we propose is the so-called reverse Monte Carlo (RMC) modeling technique, which usually relies on a particular experimental output, such as diffraction data, and combines these data with simulation techniques [5] (for reviews, see, e.g., Refs. [6,7]). The main goal of a reverse Monte Carlo calculation is to build three-dimensional structural models of a system that are consistent with diffraction data. The algorithm of the reverse MC modeling has been discussed in detail in Refs. [5–7]. It is just worth mentioning that in the RMC framework, series of configurations (sets of particle coordinates) are generated randomly. Some of the configurations are accepted in accordance with their compatibility with the experimental structure factor, $S(Q)$ (or with the corresponding "experimental" pair distribution function (pdf), $g(r)$, the inverse Fourier transform of the structure factor). This approach has been applied to simple fluids and their mixtures, to molten salts and alloys, and to hydrogen-bonded and chemically reacting fluids [8–12]. Coming closer to the present subject, RMC was applied to the study of colloidal systems, fitting the small-angle scattering signals [13,14], and also to the study of carbon aerogels, fitting the pair distribution function obtained from electron diffraction data [15].

The main point to clarify concerning the modeling is how RMC behaves when it has to deal with features that appear as (sometimes, large) inhomogeneities of the atomic scale structure and as a result, scattering intensities may be different by an order of magnitude for the small (SAS regime) and wide-angle (diffraction regime) parts of the data. During the RMC procedure, the difference between experimental and simulated structure factors (or pair distribution functions) is being minimized; if the intensity of the SAS signal is much greater than that of the wide-angle part (as expected from experience) then there is a danger that the wide-angle part, representing the atomic scale structure, will be neglected. Conversely, if modeling in the r-space is done, as in Ref. [15], it is the larger scale structure which may be underrepresented. Added to this problem, it is obvious that simulations must be applied to large systems, which may lead to a prohibitively huge number of particles in the box.

For assessing if an RMC-based scheme is feasible for achieving the main goal of considering atomic and supramolecular length scales simultaneously within one structural model, we have undertaken this exploratory study on a model system, in the spirit of Refs. [12,15,16]. In order to mimic experimental data for the structure of silica aerogels we have applied computer simulation. A particular method useful for this purpose is the so-called diffusion-limited cluster aggregation (DLCA). The model of diffusion-limited aggregation has been developed by Witten and Sander [17] (note that, strictly speaking, their method was not appropriate for colloidal systems). Diffusion-limited cluster aggregation was originally proposed for lattice models [18,19]. More recently an extension of this simulation scheme for continuous models has been applied [20]. A detailed analysis of the DLCA simulation results and comparison with the SAS experimental data for colloidal and basic aerogels has shown the validity of the simulation method to describe both the microscopic structure and larger scale correlations between big aggregates in such systems [21].

In this work the pdf coming from the DLCA simulation, according to our own code, is taken as an "experimental" result and is applied as an input for the RMC procedure. Also, the structure factor obtained as a result of the DLCA Fourier-transformed pdf is considered as the "experimental" structure factor. Both the $g_{\mathrm{DLCA}}(r)$ and $S_{\mathrm{DLCA}}(Q)$ explicitly demonstrate structural features whose interpretation requires the microscopic and larger length scale of correlations between particles forming gel structure.

In the following section, the generation of "experimental" data via the DLCA algorithm for continuous models [21] is described. We comment very briefly on the principal steps of the simulation procedure and present selected pair distribution functions obtained by our own simulations. Those are compared with the results of Hasmy et al. [21]. This part of our study as well as discussion of the model aerogel structures has original elements and besides provide better understanding of the area by the reader.

The next section is dedicated to the description of RMC modeling and to the detailed comparison of the RMC results with the DLCA-generated structures. Finally, conclusions are given and possible future developments of the method seen by us are discussed.

2. Gel structure (DLCA simulation and pair distribution functions)

The off-lattice diffusion-limited cluster aggregation (DLCA) algorithm is applied to generate gel structure via simulation. Together with reaction-limited cluster aggregation (RLCA), it is nowadays a widely used and successful method to obtain gel-like structures.

The initial configuration of the system is prepared by distributing randomly a given number of particles, N, in a cubic simulation box with edge L. The interaction between particles is irrelevant in the DLCA algorithm. However, the particles are considered to be spherical objects that cannot penetrate each other, i.e., hard spheres. Essentially, the initial configuration corresponds to nonoverlapping spheres. The diameter of particles, σ, is taken, without loss of generality, as a length unit, i.e., $\sigma = 1$. The dimensionless number density, $N\sigma^3/L$, will be denoted simply by ρ in what follows.

The initial configuration can be considered as a collection of N_a aggregates, each containing one particle. In the course of simulation one generates a collection of N_a aggregates where the ith aggregate will contain n_i particles, such that

$$\sum_{i=1}^{N_a} n_i = N. \quad (1)$$

The formation of the aggregates is performed as follows. Pick up an aggregate at random, according to the probability distribution

$$P = n_i^{\alpha} \Big/ \sum_{1 \leqslant i \leqslant N_a} n_i^{\alpha}, \quad (2)$$

where $\alpha = -0.55$ was taken to coincide with $-1/D$, where $D \approx 1.78$ is the fractal dimension of the resulting aggregates built in three dimensions.

One attempts to displace the chosen aggregate by unit length, at random in one of six directions, i.e., $\pm X$, $\pm Y$, $\pm Z$. If the cluster (aggregate) does not collide (overlap) with any other cluster during displacement step, the movement is accepted and another cluster is chosen to continue simulation. On the other hand, if the cluster, e.g., 1, overlaps with another cluster, e.g., 2, then the displacement again is accepted. However, such displacement equals to the shortest distance ensuring that one of particles belonging to the cluster 1 is tangent to any one particle of the cluster 2. Henceforth, the two clusters, 1 and 2, merge to form one cluster and the number of aggregates consequently is updated. As is common, periodic boundary conditions are used in all directions. The DLCA process terminates when a single cluster is formed. However, the box length and the number of particles must be chosen with care, to provide that the final single cluster spans the simulation box along three axes. It has been argued in Refs. [20,21] that the distribution of particles in the system can be well characterized in terms of a common pair distribution function, $g(r)$, in spite of the out-of-equilibrium structure of the formed gel. The distribution function in this simulation is calculated according to common counting [4], with grid of $\Delta r = 0.1$.

We have performed the DLCA simulation of gels at densities $\rho = 0.05$, 0.075, 0.0875, and 0.1. The box in all runs has been kept the same, $L = 50$. The box then contained 6250, 9375, 10,938, and 12,500 particles, respectively. We have performed (3 to 5) independent runs at each density to ensure reasonable statistics. Computations in such a large box are demanding in terms of computer power. Each run at given density ends up with a gel. Moreover, a set of densities *and* the box length used to obtain the pdf's provide the structures denser than the gelling threshold.

Resulting pdf's are shown in Fig. 1, in the form that was used in Ref. [22]. By comparing our results to Fig. 4 of Ref. [22], where $g(r)$'s for densities of 0.04, 0.08, and 0.12 are presented, it is clear that the two sets of data are in good agreement: the same trends are observed as a function of density, in all the three regimes (nonfractal, fractal, and intercluster) that were distinguished in Ref. [22]. According to

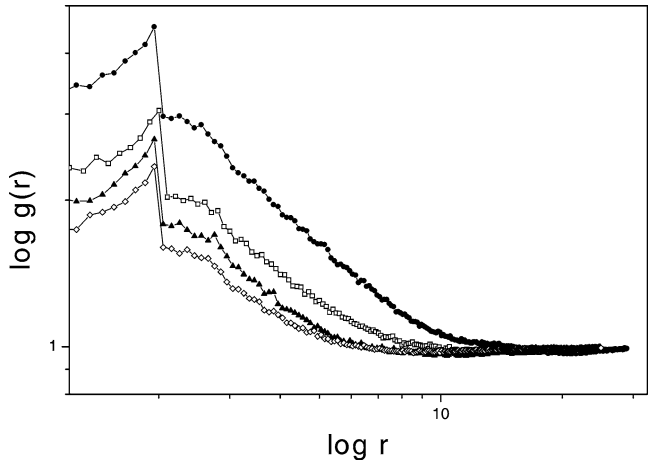

Fig. 1. The pair distribution functions, $g(r)$, of gels obtained by the DLCA simulation algorithm in the cubic box with $L = 50$. The lines with symbols from top to bottom (on the left axis) are at density $\rho = 0.05$ (full circles), 0.075 (empty squares), 0.0875 (full triangles), and 0.1 (empty diamonds), respectively. The logarithmic scale has been used to facilitate visualization of the details of the structure and comparison with the results of other authors; see, e.g., Ref. [22].

their interpretation, the nonfractal regime at low r describes the short-range shell region, and in the intercluster regime, the minimum of $g(r)$ characterizes the intercluster correlations, whereas the fractal regime can be found in between the two previous ones. The fractal regime is distinguished by the range of r where the $g(r)$ curve exhibits the most linear behavior in log–log coordinates.

In order to obtain better statistics for the pdf and also to be able to perform calculations within a reasonable amount of time, we have carried out DLCA simulations in a smaller box, $L = 40$, at our highest density, $\rho = 0.1$. In Fig. 2a, the pdf resulting from 20 independent calculations is given by the solid line. The agreement of our result with that of Ref. [21] (cf. Fig. 3 of that work) is very good. That is, the value of $g(r)$ at the first minimum, the height of the second maximum, and the value at the cusp at $r = 3$ all agree, as well as the position of the shallow minimum. A high maximum at $r = 1$ probabilistically describes contacts between particles. Also, a discontinuity at $r = 2$ is observed, which is related to the filling of the coordination sphere of dimers. The shallow minimum of the pdf characterizes the mean cluster size. For the purposes of our RMC studies, this system is convenient to deal with. It is worth mentioning that for smaller densities, particularly for $\rho = 0.05$ and less, bigger boxes must be chosen both for the DLCA simulation and for RMC modeling. As a consequence, simulations would become slow.

3. Reverse Monte Carlo modeling: results

In order to mimic experimental diffraction data we have calculated the structural properties, such as the pair distribution function as calculated from the particle configurations

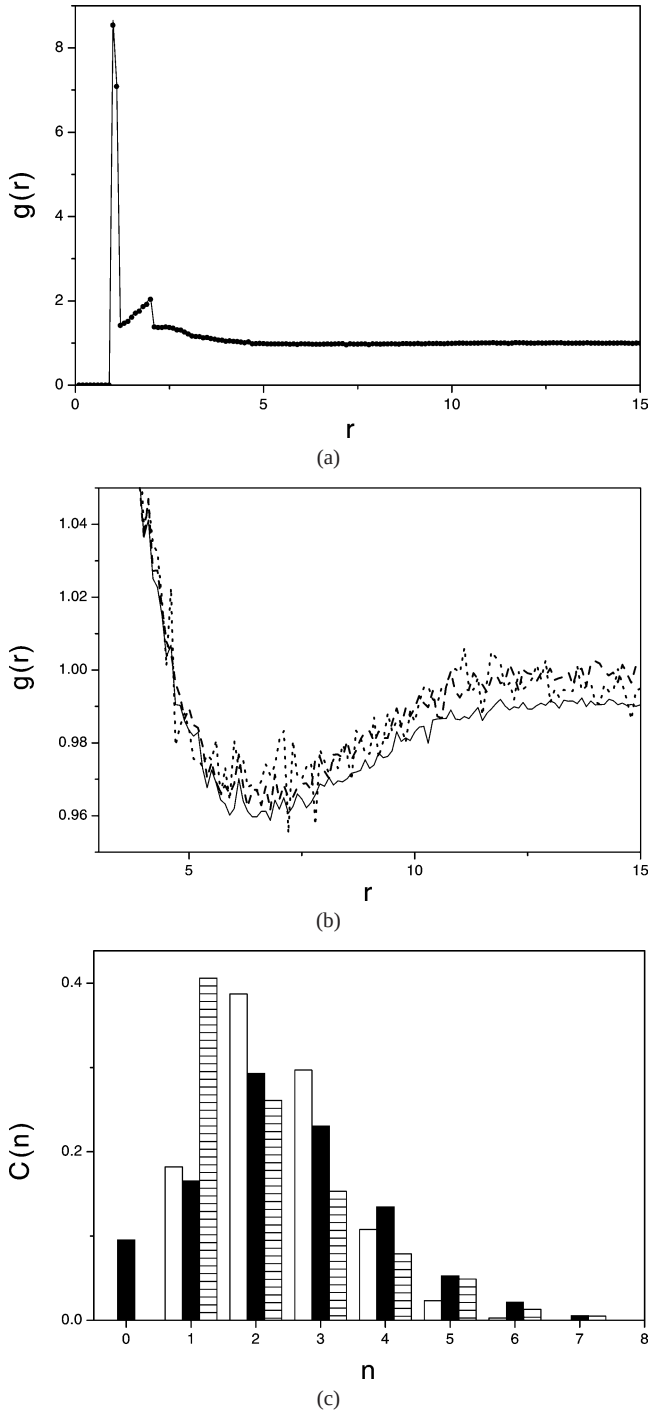

Fig. 2. (a) Reverse Monte Carlo fit with constraints (symbols) to the DLCA pdf (solid line) at $\rho = 0.1$. (b) A blowup of part (a) over a restricted r and $g(r)$ range, for emphasizing the region of the shallow minimum of the pdf. Solid line: DLCA; dashed line: RMC without constraints; dotted line: RMC with constraints. (c) Distribution of the number of neighbors for DLCA (empty bars), RMC fitting the pdf without constraints (full bars), and RMC fitting the pdf with constraints (shaded bars).

provided by the DLCA algorithm, and then its Fourier transform, the structure factor, $S(Q)$.

During the atomistic RMC procedure, each particle in the simulation box (with periodic boundary conditions) is moved according to a Monte Carlo type algorithm, accepting configurations that provide a decreasing difference between measured (experimental, or "pseudoexperimental" in the present study) and calculated (from the particle coordinates) structure factors, until this difference reaches minimum, and afterward oscillates around the minimum value. A fraction of configurations which deviate from the experimental data also are included in the course of a run. A set of (representative) configurations then can be exploited for the calculation of various structural and other properties. In the present case, the distribution of the number of first neighbors will be reported.

Most frequently, RMC is driven by the structure factor. However, one can idealize the picture by assuming that error-free ("perfect") data are available and use the pair distribution function, $g(r)$, to drive the RMC procedure. This possibility will be explored in the present study, besides the procedure utilizing the Fourier-transform as an input.

A rather useful feature of RMC is its capability for imposing coordination constraints on the structural models (for more details, see, e.g., Ref. [9]). In the following discussion of the results, if specified, one constraint was imposed so that the particles with no neighbors were not allowed to occur. Technically, this means that within a prespecified range, particles were required to have at least one neighbor. A move that resulted in a local coordination that did not satisfy this requirement was immediately rejected to avoid occurrence of free particles.

Most of the RMC calculations were carried out on the highest density system that was identical to the one used in the DLCA simulations with $\rho = 0.1$ and $L = 40$. Some calculations were performed at $\rho = 0.075$ to test the capabilities of the approach at lower densities, as well.

We start the discussion of RMC results by considering the modeling in r-space. Fig. 2a compares the pair distribution function for the DLCA system with $\rho = 0.1$ to its constrained reverse Monte Carlo fit. We have also carried out reverse Monte Carlo calculations without constraints; the pdf from that calculation was not distinguishable from the constrained one. It can be seen that RMC modeling of the $g(r)$ can reproduce every single detail of the DLCA pdf, including the first and second maxima and minima, as well as the cusp at $r = 3$.

Fig. 2b gives the same comparison as Fig. 2a, but the emphasis is placed now on the shallow minimum around $r = 6.5$, which is characteristic of the mean cluster size in the DLCA gel. At this scale, constrained and unconstrained calculations can be distinguished: the constrained one exhibits somewhat larger statistical noise than the unconstrained version. A possible explanation for this may be that algorithmically, in the fitting procedure with constraints, the emphasis is placed on the number of the nearest neighbors rather than the high-r regime. The main features above $r = 3$, the position and depth of the minimum are essentially identical for the two RMC runs and correspond very well to the DLCA-values.

Now, we wish to investigate structural features of both DLCA and RMC models beyond the level of the pair distribution function. For this purpose, the normalized *distribution* of the number of neighbors $C(n) = i_n/N$ (where i_n is the number of particles having n neighbors; recall that N is the number of particles in the box) has been calculated. Counting of neighbors is performed by the evaluation of particles in contact. This distribution is not available from the pdf; one must exploit the particle configurations. In Fig. 2c, this distribution is compared for the DLCA and RMC (with and without constraints). It is apparent that as a result of a reverse Monte Carlo run without constraints, there remained a significant fraction, about 10%, of particles with no neighbors. In a gelated system, where all the particles belong to one single cluster, the presence of solitary particles is not allowed. This was the primary reason for introducing coordination constraints into the RMC calculation and this is why, in the later stages of this work, only constrained RMC calculations will be considered.

The average number of neighbors, $\bar{n} = \sum C(n)n$, has a value of 2.4 (DLCA). From this, one may expect that two- and threefold coordinated particles are most likely to be present. Indeed, this is the case, as follows from Fig. 2c. What is interesting is that the DLCA algorithm results in a high concentration of onefold particles. This seems to be a manifestation of the developed surface of blobs and its "hairy" shape. On the other hand, we have seen already that the minimum of the distribution function is shallow, such that the distribution of cluster sizes is expected to be wide. The highest coordination number that is found in the DLCA-structure is 6, with a frequency of about 0.3%.

As it was mentioned above, the unconstrained RMC calculation produces a nonnegligible fraction of neighborless particles and, therefore, it has to be abandoned. However, the occurrence of one-, two-, and threefold coordinated particles in the unconstrained model is in better agreement with DLCA results than with those in the constrained RMC model. This indicates that the constrained RMC algorithm, when applied with only one constraint, the one that prohibits the presence of nonbonded particles, is too crude for the reproduction of the finer details of the structure: the number of onefold coordinated particles should also be restricted. This has been attempted by applying two coordination constraints, with moderate success: in that case, it was not possible to make the zerofold coordinated particles vanish. The highest coordination number found in the RMC models was 11, but only particles with seven neighbors (or fewer) appeared with a frequency higher than 0.1%. The average coordination number is 2.3, which agrees within 5% with the DLCA value. The occurrence of five-, six-, and sevenfold coordinated particles is much higher in the RMC models than in the DLCA system. One should have in mind that our analysis is based on a single configuration for DLCA gel and single RMC configuration, both yielding reasonable $g(r)$. We have not performed such an analysis for several configurations and have not performed averaging. However,

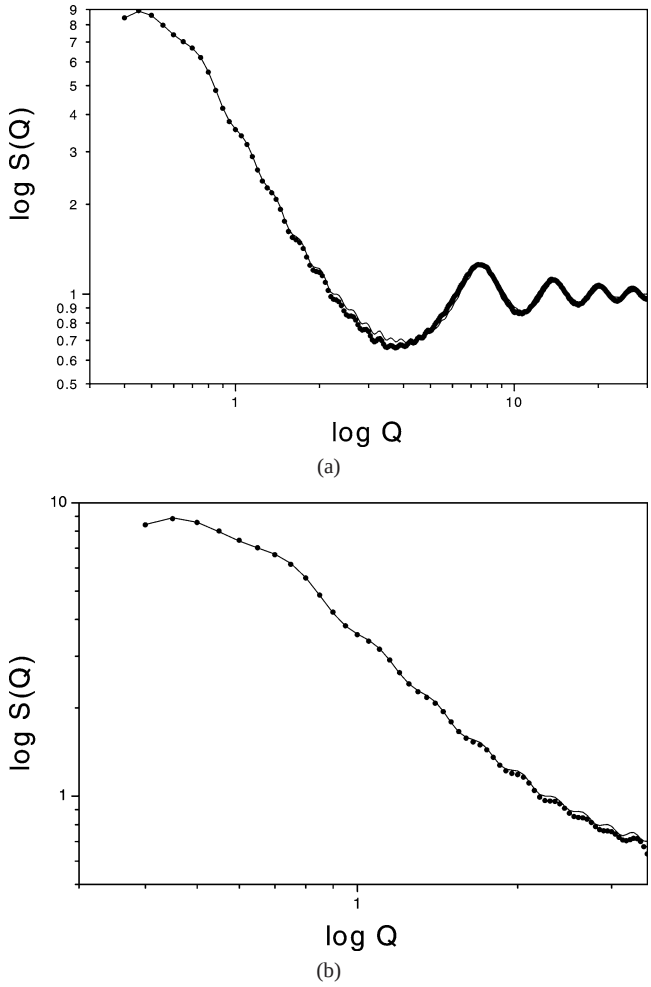

Fig. 3. (a) Reverse Monte Carlo fit with constraints (symbols) of the structure factor for the DLCA model at $\rho = 0.1$ (solid line) over the entire scattering vector range, comprising both the small and the wide angle scattering regions. (b) Same as (a), but fitting the small-angle scattering region only. (Note the logarithmic scale for both parts.)

the large size of the box and large number of particles involved permit us to conclude that the observed behavior is reasonable.

The next step was the application of the structure factor as input for the reverse Monte Carlo algorithm. The $S(Q)$ was obtained by Fourier transformation of the (DLCA) pair distribution function, using the same minor correction for accounting for the deviation of the plateau value of the $g(r)$ from unity as in Ref. [21]. This allowed us a similar extension of the $S(Q)$ toward smaller scattering vector values [21]. Key features of the structure factor (see Fig. 3a), i.e., positions and $S(Q)$ values of maxima and minima, as well as the overall shape, are in excellent agreement with previous work on a system with very similar density, cf. Fig. 6 of Ref. [21]. We would like to note that Fourier transformation was carried out on pdf's calculated only up to distances smaller than half of the box size. In this way, any conceivable effects of periodic boundary conditions could be avoided, since no correlations were considered between

any particle and its image. Fourier transformation of the pdf over finite r-ranges may lead to truncation errors; these may be minimized by choosing large simulation boxes (as it is done here).

As it can be seen in Fig. 3a, RMC modeling (with constraints) of the (DLCA) structure factor provides very good coincidence with the "experimental" $S(Q)$, over the entire scattering vector range. Remember that in practice, no experiment can provide similar coverage of the reciprocal space—one would need a SAS and a conventional diffraction experiment to obtain the structure factor shown in Fig. 3a.

For (aero)gels, it is the small-angle scattering experiment that has been carried out the most frequently; see, e.g., Refs. [21,23–25]. For this reason, the "small-angle scattering" part of the DLCA structure factor has been constructed, cutting the full $S(Q)$ (Fig. 3a) at the position of its first minimum at $Q = 3.5$, and considering the region only below this point. The RMC modeling of this "SAS $S(Q)$" has also been performed, with the aim of establishing to what extent the SAS region of the full structure factor can account for the structural properties of a DLCA gel. Fig. 3b displays the excellent agreement between DLCA and RMC (performed with constraints) small angle scattering $S(Q)$s.

A most stringent test of the reverse Monte Carlo approach can be undertaken by comparing the pair distribution functions resulting from fitting the (full and SAS) structure factor(s) to the original DLCA pdf. This test would indicate how well a given "gel-like" structure can be deduced on the basis of scattering experiments. Such a comparison is made in Figs. 4a and 4b, the former concentrating on the region of the second maximum, around $r = 2$, whereas the latter shows the region of the shallow minimum, around $r = 6.5$.

Around the second maximum, RMC modeling of the full structure factor reproduces the DLCA curve satisfactorily, including the singularity points. Modeling only the SAS part fails to retrieve these important features with the desired accuracy, although the position of the second maximum and the cusp at $r = 3$ are approached qualitatively, in a spread-out manner. Fig. 4a may be taken as an indication that small-angle scattering data alone are not sufficient for a meaningful description of the short-range part of the pdf. Above $r = 3$, the two RMC curves run together with the DLCA $g(r)$, through the shallow minimum and up to about $r = 10$. One may also note that the pdf from fitting the SAS part only clearly exhibits a higher level of statistical noise, in accordance with the notion that this function is less well determined comparing with the pdf by fitting the full $S(Q)$.

The distribution of coordination numbers was also calculated for the structure factor based RMC models. A comparison between histograms for DLCA, $g(r)$-based RMC (with constraints), and full $S(Q)$-based RMC (with constraints) is provided by Fig. 4c. Note that even though the onefold coordinated particles are still overrepresented, agreement with DLCA results is significantly better for the structure-factor-based RMC model.

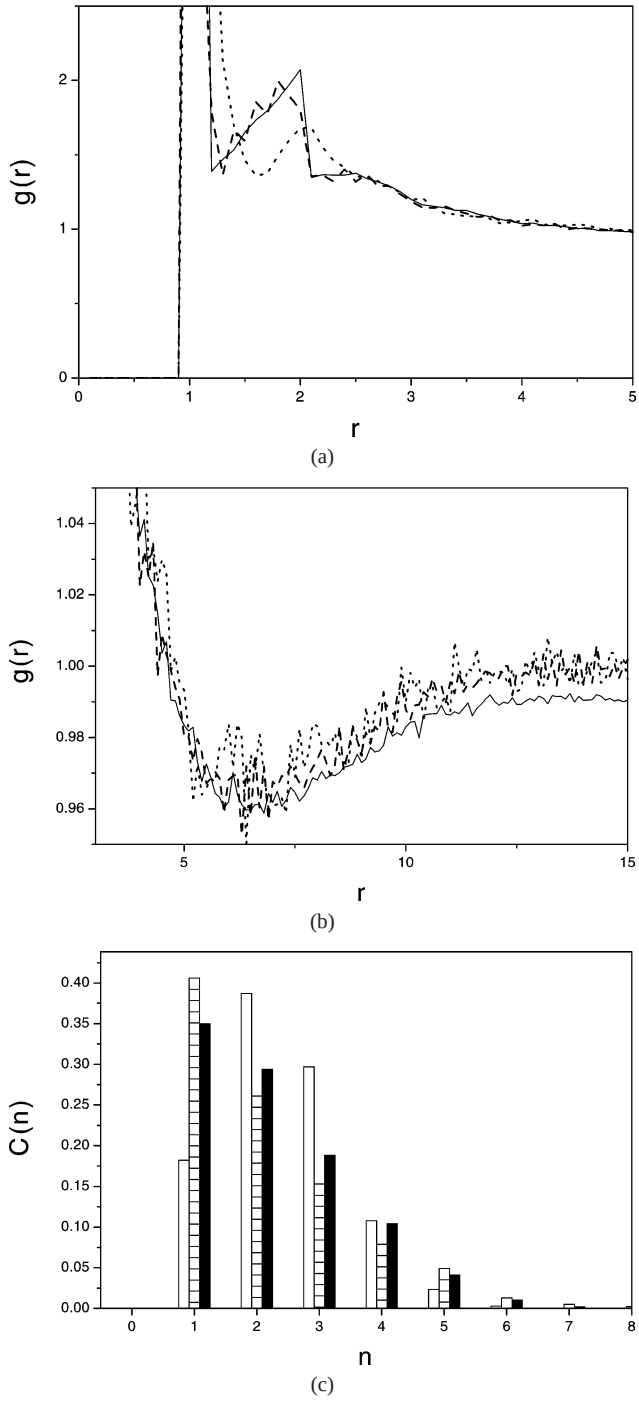

Fig. 4. (a) Pair distribution functions as derived from RMC modeling of the entire $S(Q)$ (dashed line) and of the small-angle scattering part of the $S(Q)$ (dotted line), as compared to the pdf of the DLCA model (solid line) at $\rho = 0.1$. (b) Same as part (a), but emphasizing the region of the shallow minimum of the $g(r)$. (c) Comparison of the distribution of the number of neighbors for the DLCA model at $\rho = 0.1$ (empty bars), for the model resulting from RMC modeling the pdf of the DLCA model, with constraints (shaded bars) and for the model resulting from RMC modeling the structure factor of the DLCA model, with constraints (full bars).

In order to demonstrate the applicability of the reverse Monte Carlo approach at lower densities, the DLCA gel with $\rho = 0.075$ was also considered. In Fig. 5a, the RMC fit (with

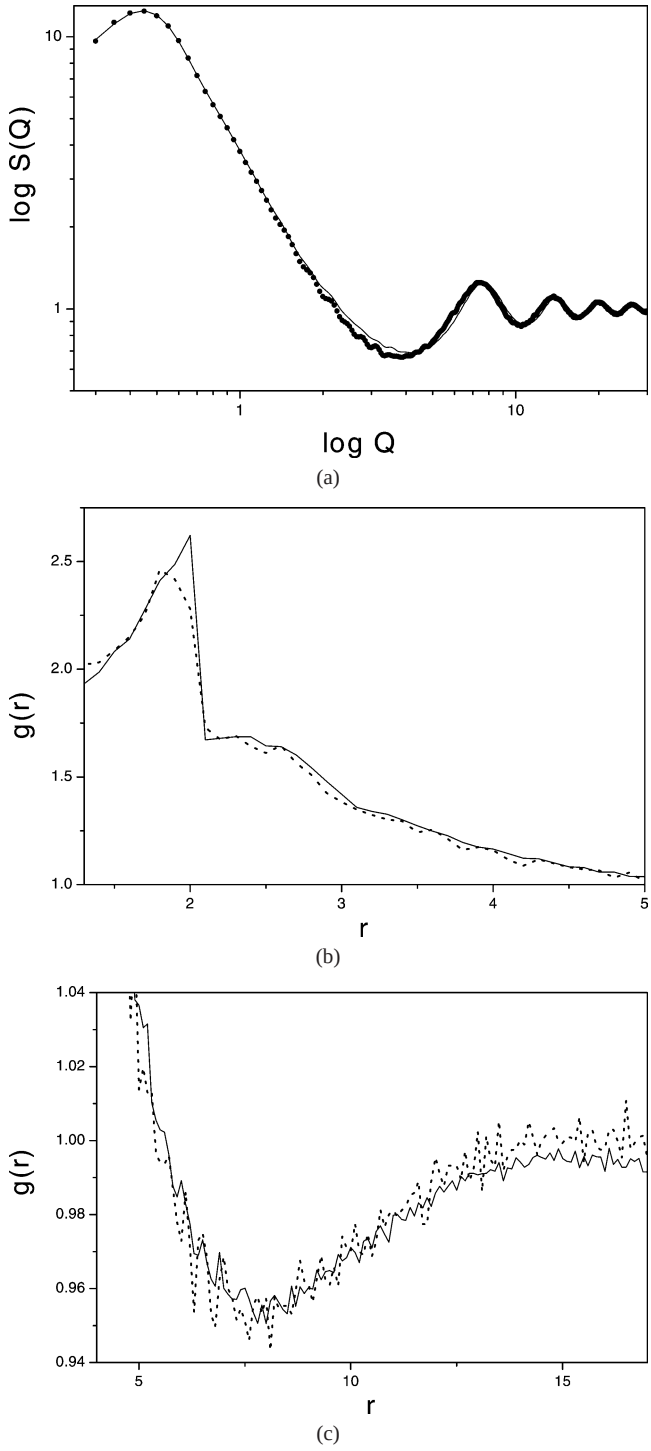

Fig. 5. (a) Reverse Monte Carlo fit with constraints (symbols) of the structure factor for the DLCA model at $\rho = 0.075$ (solid line) over the entire scattering vector range. (b) Pair distribution function as derived from RMC modeling of the entire $S(Q)$ (dotted line), as compared to the pdf of the DLCA model at $\rho = 0.075$, emphasizing the region of the second maximum of the $g(r)$. (c) Same as (b), but emphasizing the region of the shallow minimum of the $g(r)$.

constraints) to the full structure factor is compared to the DLCA $S(Q)$ at this lower density. The agreement is nearly as good as for the higher density case, even though there have been many indications (see, e.g., Ref. [12]) that the RMC algorithm usually finds greater difficulties when fitting sharp features (such as the contact value and second maximum of DLCA pdfs) at lower density. The pair distribution function resulting from fitting the DLCA $S(Q)$ is compared to the DLCA pdf in Fig. 5b (low r) and 5c (high r). Again, the reproduction of important sharp features (second maximum and minimum) is nearly as successful as it was at $\rho = 0.1$, as can be seen in Fig. 5b.

4. Concluding remarks

It is demonstrated that by means of the reverse Monte Carlo method for structural modeling, it is possible to retrieve important properties of a gel-like structure that had been prepared by DLCA. Since it is commonly accepted that diffusion-limited cluster aggregation provides a good model for the structure of colloidal and basic aerogels [21], we suggest that the RMC approach can provide an equally good representation of the aerogel structure. The advantage of RMC, however, is that it can be applied directly to the experimental structure factor.

It was also shown that for a DLCA structure, the wide-angle region of the structure factor contains important information, particularly about features of the pdf at low r values. It is suggested that the SAS region is insufficient for a proper characterization of the small scale structure, i.e., in the non-fractal region. Larger scale features (the fractal region and intercluster correlations), on the other hand, are described with appropriate accuracy. To further clarify this issue, neutron diffraction experiments at the Budapest Research Reactor (Hungary) on different silica gels are underway.

Very recently, it has been proposed that for the accurate determination of the fractal dimension from SAS data, one has to have the pair distribution function of the system in question [22]. We suggest that for this purpose, the reverse Monte Carlo method may serve as convenient and reliable tool with similar accuracy.

Throughout the present work, the RMC algorithm applied moves of individual particles only. An important future extension of the algorithm may be the introduction of movements of clusters, in a similar manner as it is done in the DLCA method. This development seems to be necessary for creating fully connected networks of particles.

For porous materials, like silica aerogels, the characterization of the network of pores is perhaps as important as the characterization of the network of particles. For this purpose, it may be feasible to apply the particle insertion method described in Ref. [26] for the models prepared by either DLCA or RMC. This may enhance our understanding of the structure of silica aerogels.

Finally, it has to be mentioned that almost all real colloidal systems have some degree of polydispersity; for this reason, a more elaborated code will have to deal with this

difficulty. One possible way is to change the particle diameters during the RMC calculation, in the fashion of Ref. [14].

Acknowledgments

L.P. thanks the Eötvös Travel Grant scheme of the Hungarian Ministry of Education. This work was supported by the Hungarian Academy of Sciences and the CONACyT of Mexico, via the bilateral project E130.377/002. H.D. and O.P. acknowledge support under Grants CONACyT (Mexico) 37323E and DGAPA (UNAM, Mexico) IN113201. Financial support for L.P. by OTKA—Hungarian Basic Research Fund (Grant T42495) is also acknowledged.

References

[1] L.A. Feigin, P.I. Svergun, Structure Analysis by Small Angle X-Rays and Neutron Scattering, Plenum, New York, 1987.
[2] G.L. Squires, Introduction to the Theory of Neutron Scattering, Dover, New York, 1996.
[3] J.C. Dore, M. Sliwinski, A. Burian, W.S. Howells, D. Cazorla, J. Phys. Condensed Matter 11 (1999) 9189.
[4] M.P. Allen, D.J. Tildesley, Computer Simulation of Liquids, Clarendon, Oxford, 1987.
[5] R.L. McGreevy, L. Pusztai, Mol. Simulation 1 (1988) 359.
[6] R.L. McGreevy, J. Phys. Condensed Matter 13 (2001) R877.
[7] L. Pusztai, J. Non-Cryst. Solids 227–230 (1998) 88.
[8] G. Tóth, A. Baranyai, J. Chem. Phys. 114 (2001) 2027.
[9] M.A. Howe, R.L. McGreevy, L. Pusztai, I. Borzsák, Phys. Chem. Liquids 25 (1993) 205.
[10] R.L. McGreevy, L. Pusztai, Proc. R. Soc. London Ser. A 430 (1990) 241.
[11] L. Pusztai, Phys. Rev. B 60 (1999) 11,851.
[12] L. Pusztai, H. Dominguez, O. Pizio, Physica A 316 (2002) 65.
[13] G. Tóth, L. Pusztai, J. Phys. Chem. 96 (1992) 7150.
[14] G. Tóth, Langmuir 15 (1999) 6718.
[15] K.T. Thomson, K.E. Gubbins, Langmuir 16 (2000) 5761.
[16] L. Pusztai, G. Tóth, J. Chem. Phys. 94 (1991) 3042.
[17] T.A. Witten, L.M. Sander, Phys. Rev. Lett. 47 (1981) 1400.
[18] P. Meakin, Phys. Rev. Lett. 51 (1983) 1119.
[19] M. Kolb, R. Botet, R. Jullien, Phys. Rev. Lett. 51 (1983) 1123.
[20] A. Hasmy, M. Foret, J. Pelous, R. Jullien, Phys. Rev. B 48 (1993) 9345.
[21] A. Hasmy, E. Anglaret, M. Foret, J. Pelous, R. Jullien, Phys. Rev. B 50 (1994) 6006.
[22] M. Lattuada, H. Wu, A. Hasmy, M. Morbidelli, Langmuir 19 (2003) 6312.
[23] T. Freltoft, J. Kjems, S.K. Sinha, Phys. Rev. B 33 (1986) 269.
[24] D.W. Schaefer, K.D. Keefer, Phys. Rev. Lett. 56 (1986) 2199.
[25] D. Posselt, J.S. Pedersen, K. Mortensen, J. Non-Cryst. Solids 145 (1992) 128.
[26] S. Gavalda, K.E. Gubbins, Y. Hanzawa, K. Kaneko, K.T. Thomson, Langmuir 18 (2002) 2141.